Optical Spectra of Carbon-Based Nanostructures

M. Rohlfing

published in

NIC Symposium 2016
K. Binder, M. Müller, M. Kremer, A. Schnurpfeil (Editors)

Forschungszentrum Jülich GmbH,
John von Neumann Institute for Computing (NIC),
Schriften des Forschungszentrums Jülich, NIC Series, Vol. 48,
ISBN 978-3-95806-109-5, pp. 249.
http://hdl.handle.net/2128/9842

Optical Spectra of Carbon-Based Nanostructures

Michael Rohlfing

Institut für Festkörpertheorie, Universität Münster, Germany
E-mail: Michael.Rohlfing@wwu.de

Carbon exists in many forms, including zero-dimensional fullerenes, one-dimensional nanotubes, two-dimensional graphene and three-dimensional graphite and diamond. Electronic and optical spectroscopy are important tools to analyse these structures and their properties. Here we present optical spectra from *ab initio* many-body perturbation theory for nanotubes and graphite. The data allow to understand details of excited states in these materials. This is of great significance for the interpretation of experimental spectroscopy and for the future manipulation and tuning of optical properties of materials.

1 Introduction

Optical spectroscopy of carbon-based materials is an active field of research, both for fundamental reasons and for practical purposes. On the side of fundamental research, comparison of theoretical and computational results with data from experimental spectroscopy allows to identify general mechanisms of electronic-structure properties inside the material, and may allow to identify materials, defects, dopants, and other details of nanostructured systems. On the side of practical applications, computational spectroscopy might guide experiment in the preselection of materials and systems, to search for new materials and geometries, and to exclude useless systems, before going into the demanding process of sample preparation. Furthermore, theory might demonstrate and elucidate novel mechanisms in the design and control of optical excitations, like e.g. the red-shift tuning of transitions inside a carbon nanotube by touching it with other material (see below).

Internally, optical transitions involve excitons, i.e. coupled excitations of electrons and holes in the material's band structure. Excitons occur everywhere in semiconducting and insulating materials (crystals and molecules) in any dimension, and their interrelation with photons is at the heart of all optics and optoelectronics, including photovoltaics, photocatalysis and more.

Excitons in carbon nanotubes (CNT) and in graphite and graphene have become a highly active research field, providing deep insight in light-matter interaction in carbon-based materials[1–6]. In addition to the optical spectra of single CNT or a single sheet of graphene, their modification by interaction with the environment constitutes an interesting field of research. In the case of nanotubes, characteristic measurements were performed, e.g., on CNT in nitrogen atmosphere[3] and on pairs of CNT, with two CNT running along each other[4]. In both cases, a red-shift of the optical transitions to lower excitation energy was observed. In the case of graphene, the excitations inside one sheet start to interact with each other when graphene sheets are stacked to form graphite, followed by spectral changes. Here we take these observations as a motivation for a theoretical study to elucidate the physical mechanisms of spectral shifts. There are two mechanisms involved. On the one hand, the incorporation of additional polarisability (e.g., from a neighbouring nanotube or from the additional graphene sheets inside graphite) cause redshifts of the

optical excitations. On the other hand, there are exciplex contributions that do not occur in a single nanotube or graphene sheet. An exciplex (or charge-transfer) configuration consists of an electron and a hole on different components of the system, i.e. on the two nanotubes in a nanotube pair or on neighbouring sheets in graphite. The admixture of these configurations also lowers the excitation energy, but requires perfect coherence of the quantum-mechanical degrees of freedom. This is in fact given in graphite, but difficult to achieve in two adjacent nanotubes that might be slightly rotated or shifted relative to each other and may not even have the same chirality. Therefore we consider this second mechanism as relevant for graphite, but not for a pair of nanutubes in which the polarisability effect is the only significant effect of spectral shifts. We investigate all issues within many-body perturbation theory (MBPT)[7], notably by employing the GW approximation (GWA) and the Bethe-Salpeter equation (BSE)[9], which has become the standard approach for describing CNT excitons[10–13] and has also been employed for graphene and graphite.

2 Theory

In this section we briefly discuss the computational method used in this work. For a more extended discussion we refer the reader to Ref. 14.

Ab initio quasiparticle (QP) band structures result from the electron self-energy operator $\Sigma(E)$. The state-of-the-art approach to Σ is given by Hedin's GW approximation[7], which is usually evaluated and employed on top of an underlying density-functional theory (DFT) calculation. The typical procedure employs DFT data to generate the single-particle Green function G_1 and the screened interaction W (usually within the random-phase approximation). Thereafter, the resulting self-energy operator $\Sigma = iG_1W$ replaces the DFT exchange-correlation potential, V_{xc}, arriving at a QP Hamiltonian of

$$\hat{H}^{QP} := \hat{H}^{DFT} + iG_1W - V_{xc} \quad . \tag{1}$$

Eq. 1 yields qusiparticle (QP) states $|m, \mathbf{k}\rangle$ and related band-structure energies $E_{m,\mathbf{k}}$.

Based on the QP states and energies correlated electron-hole states

$$|S\rangle = \sum_{\mathbf{k}} \sum_{v}^{hole} \sum_{c}^{elec} A^S_{vc\mathbf{k}} |v, \mathbf{k}\rangle |c, \mathbf{k}+\mathbf{Q}\rangle \tag{2}$$

are considered as linear combinations of interband transitions between valence band v and conduction band c at wave vector $\mathbf{k}$. In here, $\mathbf{Q}$ is the total momentum of the electron-hole state which, in optical processes, corresponds to the momentum of the involved photon.

The ansatz of Eq. 2 leads to the Bethe-Salpeter equation (BSE)

$$(E^{QP}_{c,\mathbf{k}+\mathbf{Q}} - E^{QP}_{v,\mathbf{k}}) A^S_{vc\mathbf{k}} + \sum_{\mathbf{k}'} \sum_{v'}^{hole} \sum_{c'}^{elec} \langle vc\mathbf{k}|K^{eh}|v'c'\mathbf{k}'\rangle A^S_{v'c'\mathbf{k}'} = \Omega_S A^S_{vc\mathbf{k}} \quad , \tag{3}$$

with $E_{m,\mathbf{k}}$ being the QP energies from Eq. 1 and K^{eh} being the electron-hole intraction. The Bethe-Salpeter equation and the nature of the resulting states and spectra has been discussed extensively in the literature.

GW/BSE calculations commonly employ the random-phase approximation for evaluating dielectric screening properties (i.e., the W in the self-energy operator and the corresponding electron-hole interaction kernel). This procedure is very time consuming. For the

issues addressed in this work, a simplified, perturbative "LDA+GdW" version of MBPT is equally appropriate and much more efficient to evaluate[14,15]. While being somewhat less accurate (on an absolute energy scale) than a full GW/BSE calculation with RPA dielectric screening, LDA+GdW still fully incorporates all relevant aspects of the screening (atomistic resolution, local-field effects, and non-locality). Our reference calculations within the conventional GW/BSE/RPA approach confirms the applicability of LDA+GdW.

Note that the screened interaction W depends strongly on the environmental conditions due to the long-ranged nature and non-locality of Coulomb-interaction effects. Simply speaking, a charge at position $\mathbf{r}$ causes an electric field at position $\mathbf{r}'$. If there is material at position $\mathbf{r}'$, its electronical polarizability yields an induced charge, which in turn will generate a change of the electric fields at position $\mathbf{r}$ and therefore change the properties of the screened Coulomb interaction W. Via the self energy operator in Eq. 1, $\Sigma = iG_1W$, this long-range mechanism affects the single-particle energy levels at $\mathbf{r}$. Prominent examples include image-potential effects of molecules on metallic substrates.

A red-shift of the (optical) gap due to the spatial vicinity to a polarisable object has often be interpreted as resulting from a weakening of the (GW) self-energy operator: an increase of dielectric screening weakens W, and the gap closes. For a molecule on a metal, this would be just the image-potential effect. Similarly, a blue-shift of excitons due to the spatial vicinity to a polarisable object is sometimes interpreted as resulting from the weakening of W, as well: the attractive electron-hole interaction becomes smaller, and the exciton binding energy is reduced. It is worth to note that both effects (reduction of the fundamental gap and reduction of the electron-hole binding energy) are real, but are (to first order) exactly opposite in size, thus cancelling each other, provided that the additional polarisability is homogeneous (e.g., a simple dielectric background completely given by a dielectric constant).

Non-zero spectral shifts of excitons require that the additional polarisability be inhomogeneous. This is in fact given for many systems, e.g. the additional polarisability from a neighbouring nanotube or from an adjacent graphene sheet in graphite. It should also be noted that in such situations, model approaches like solvent models that are common in quantum chemistry to describe molecules in solution might not be applicable due to the non-locality, inhomogeneity and anisotropy of the additional polarisability. Our MBPT approach, on the other hand, fully accounts for all these effects automatically, without further effort or modelling, since the full W (being inhomogeneous, anisotropic and non-local) is a key ingredient for the QP energies as well as for the BSE.

3 Results for Nanotubes and for Graphite

For illustration we briefly discuss prototypical results for the optical spectrum of two examples of carbon-based materials, i.e. a semiconducting carbon nanotube and graphite. Carbon nanotubes are formed from a single sheet of graphene (i.e., one monolayer of graphite material) which is rolled into a tube. Depending on the geometrical details (in particular, the chirality), the tubes are metallic or semiconducting. In particular the semiconducting carbon nanotubes show one-dimensional semiconductor physics, i.e. a one-dimensional band structure with a fundamental gap and the formation of excitons across the gap. The corresponding optical transitions start at energies of around 1 eV and above, with a trend to shift to lower energies for tubes of larger diameter[8].

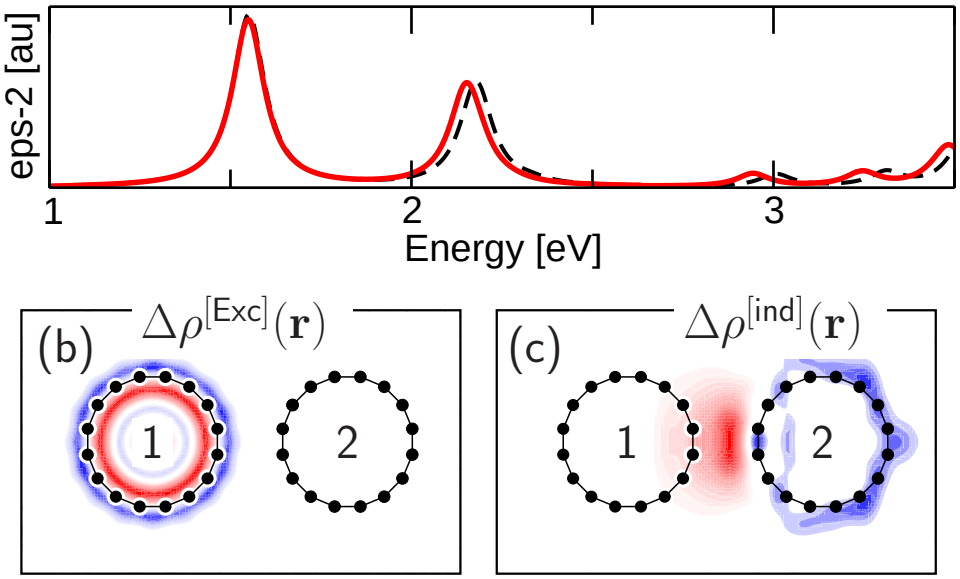

Figure 1. (a) Optical spectrum of a single (8,0) carbon nanotube. The dashed line shows the spectrum of the tube in vacuum. The solid line shows the spectrum in the vicinity of a second nanotube at van der Waals distance. The second nanotube runs along the first one and contributes environment polarisability, only. In all cases the orientation of the electric field vector is along the nanotube. (b) Charge distribution $[\Delta\rho^{[Exc]}(\mathbf{r}) := \rho_v(\mathbf{r}) - \rho_c(\mathbf{r})]$ of exciton D from panel a (blue: negative charge, red: positive charge). (c) Induced charge distribution on the other CNT (blue: negative charge, red: positive charge).

Optical spectra for an individual (8,0) CNT are shown in Fig. 1 a (upper panel). The first four optically active excitations are found at 1.55 eV, 2.18 eV, 2.33 eV, and at 3.01 eV. These results, that were obtained from the simplified LDA+GdW approach, differ slightly from our full GW/BSE/RPA reference calculation, which yields 1.60 eV, 2.05 eV, 2.42 eV and 3.16 eV for the four peaks. A previous GW/BSE/RPA calculation[10] yielded 1.55 eV and 1.80 eV in comparison with experimental data of 1.60 eV and 1.88 eV[1,2]. The slight deviations of our LDA+GdW data result from the approximations involved and from the employment of a model screening.

Starting from the dashed-line spectra of Fig. 1, we now include in the screening the polarisability of another nanotube. In experimental situations the two nanotubes stick to each other due to attractive van der Waals interaction, which makes them lie side by side. If more tubes are involved this would finally result in a bundle. Here we focus on just two nanotubes, both of which are supposed to be (8,0) tubes. The solid line in Fig. 1 shows the effect on a (8,0) CNT when another (8,0) tube is attached to it (at a distance of 3.15 Å). All peaks are redshifted to lower excitation energy. Note that the redshifts are significantly smaller than the reduction of the fundamental gap and of the exciton binding energy (both $\sim$0.3 eV). Both effects largely cancel each other (provided that they are described on equal footing, as in our present realisation of MBPT), yielding only a small net effect of a few meV. Our full GW/BSE/RPA reference calculation yields the same redshifts to within 10 meV.

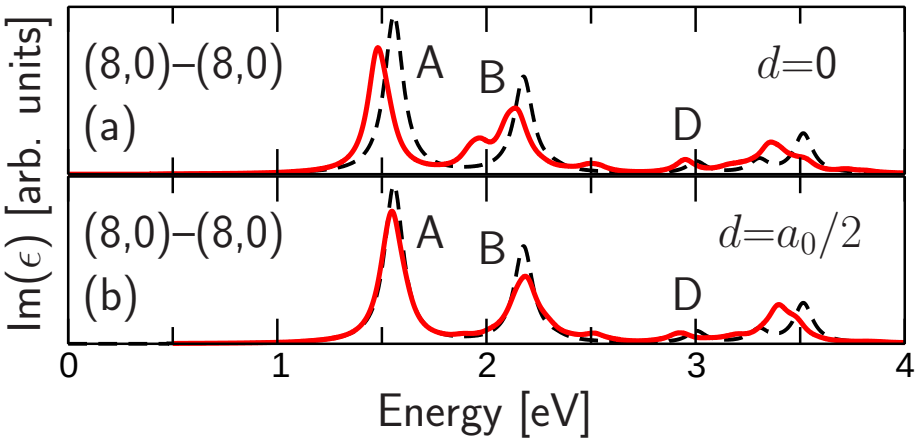

Figure 2. Effect of *electronic coupling* between two (8,0) CNT on their spectra. (a) The two CNT run along each other, with no spatial shift between their unit cells. (b) The two CNT are shifted relative to each other (along their axis) by 2.1 Å (i.e., one half of their lattice constant). In both panels the dashed curve indicates the spectrum of a single CNT in vacuum (cf. Fig. 1).

The redshift results from the polarisation of CNT 2 when an exciton on CNT 1 is excited[16]. As illustration, Fig. 1 b shows the change of electronic charge [$\Delta\rho^{[Exc]}(\mathbf{r}) := \rho_v(\mathbf{r}) - \rho_c(\mathbf{r})$] when exciton D is excited on CNT 1. Since the conduction (c) states are closer to the vacuum level than the valence (v) states, the former extend farther into the vacuum, causing $\Delta\rho(\mathbf{r})$ to be slightly positive inside CNT 1 and slightly negative outside. This slight inhomogeneous charge distribution of the exciton leads to a polarisation of the material nearby (here: CNT 2), as shown in Fig. 1 c [induced charge density $\Delta\rho^{[\mathsf{ind}]}(\mathbf{r})$]. The interaction between $\Delta\rho^{[Exc]}(\mathbf{r})$ and $\Delta\rho^{[\mathsf{ind}]}(\mathbf{r})$ finally redshifts the excitation.

Note that such effects are particularly important if $\Delta\rho^{[Exc]}(\mathbf{r})$ is non-zero at such positions $\mathbf{r}$ where system 2 has high charge susceptibility (caused by its own electronic structure) and inhomogeneity. This is mostly the case at distances of about 1-3 Å from the nuclei of system 2. Here system 2 can be polarised by $\Delta\rho^{[Exc]}(\mathbf{r})$ even if it carries no dipole. For any exciton, $\Delta\rho^{[Exc]}(\mathbf{r})$ must be non-zero somewhere (if not simply for the above-mentioned argument that electrons extend farther into vacuum than holes). The effect described here should thus be of widespread relevance.

In addition to the influence of environmental polarisability, as discussed above, another effect occurs between two touching CNT: the admixture of exciplex (or charge-transfer) configurations to the excitons. For a single tube in vacuum, the electron and the hole have to reside on just the one CNT. For two touching CNT, there are configurations in which the electron is on one CNT and the electron on the other (and vice versa). Simple considerations from second-order perturbation theory indicate that this extension of the configurational space yields an energetic downshift of all excited states, i.e. red-shift trends. This is confirmed by our results shown in Fig. 2 which exhibits the spectrum of a pair of CNT (solid line) in comparison to the spectrum of a single CNT (dashed line). However, this effect of exciplex admixture depends very sensitively on geometric details of the interface. For example, a sliding shift of 2.1 Å (i.e., half a lattice constant) of one tube relative to the

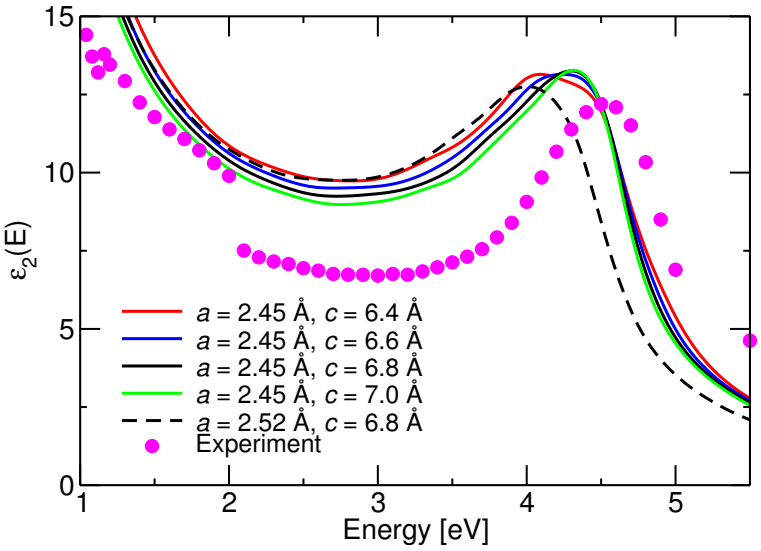

Figure 3. Imaginary part of the dielectric function of graphite, calculated for various values for a and c. Experimental data from Ref. 17.

other completely changes the redshifts (while still being small), as shown by the difference between the two spectra in Fig. 2 a and b. Similar sensitivity was observed for rotations of the CNT around its axes, even for smallest angles[8]. Apparently, imperfect coherence between the electronic (or hole) orbitals of the two components causes uncontrollable scattering of the redshift (while, however, always being negative). Further "chaotic" behaviour of these effects can be expected if the two CNT have different chirality, as in experimental situations. Therefore we conclude that the exciplex admixture is not relevant for CNT, while the environmental polarisability effects is found to be very stable against geometrical details[8].

The situation in graphite, while being composed of the same graphene sheets from which the nanotubes are formed, is nonetheless significantly different. In particular, the graphene sheets are flat instead of rolled up, and the stacking of the sheets adds three-dimensional character to the material. As a consequence of the different structure, graphite has no fundamental band gap. The optical spectrum can, however, again fully be described by GW-BSE[18–23], with self-energy effects and electron-hole attraction similar to semiconductors, as demonstrated by Yang *et al.*[23]. Within LDA+GdW we obtain a spectrum (see Fig. 3) in good agreement with the GW-BSE study by Yang *et al.*, with a maximum at 4.30 eV (4.50 eV in GW-BSE[23]) which is 0.32 eV lower than in the free interband spectrum (0.27 eV in GW-BSE[23]) due to electron-hole attraction. Here we focus on the dependence of the spectrum and of the contributing excitons on the lattice constants a and c around the experimental equilibrium of a_0 = 2.45 Å and c_0 = 6.71 Å. Fig. 3 shows the LDA+GdW optical spectrum for various combinations of a and c. For increasing c the peak near 4.3 eV shifts to higher energies (by about 0.3 eV/Å). The spectrum (including the peak at 4.3 eV) is formed from a large number of resonant rather than bound excitonic states. Changes

in the spectrum do not only result from changes in the excitation energy of each exciton, but also from changes in their optical dipole strength. Between 1 eV and 2 eV, for instance, the spectrum seems to be shifted towards *lower* energy for increasing c. A closer analysis of our data, however, shows that each exciton is rather shifted towards *higher* energy for increasing c. Note that for the graphite case, both the environmental polarisability effect and the admixture of exciplex configurations contribute to the above mentioned spectral shifts. Different from the case of two touching CNT, neighbouring sheets in graphite form a perfect match and allow for wave-function coherence over large distances, thus forming the perfect phase-matching conditions for electrons and holes which is necessary for redshifts from charge-transfer configurations.

4 Summary

In conclusion, we have shown that electronic polarisability of neighbouring systems can redshift exciton states of carbon nanotubes. Here the exciton's charge-density distribution induces charge density in the neighbouring system. This mechanism is particularly effective when the excited system is very close to the neighbouring system, e.g. at physisorption distance. This should be relevant not only for carbon nanotubes (which were taken as an example in the present study), but also for other molecules, polymers, etc. in contact with chemically inert systems. In addition to the polarisability effect, electronic coupling between the systems can significantly enhance the redshifts. However, very precise control of the contact structure would be required for electronic coupling, since it depends very sensitively on the atom positions of the two components relative to each other. For two touching CNT, this condition is not given. In contrast, graphite shows such perfect matching between the sheets that electronic coupling is equally relevant. Both systems demonstrate the delicate relationship between structure and spectra of nanoscale systems.

Acknowledgements

The author gratefully acknowledges the computing time granted by the John von Neumann Institute for Computing (NIC) and provided on the supercomputers JUROPA and JURECA at Jülich Supercomputing Centre (JSC).

References

1. S. M. Bachilo *et al.*, Science 298, 2361 (c022002).
2. R. B. Weisman and S. M. Bachilo, Nano Lett. 3, 1235, 2003.
3. P. Finnie *et al.*, Phys. Rev. Lett. **94**, 247401, 2005.
4. F. Wang *et al.*, Phys. Rev. Lett. **96**, 167401, 2006.
5. F. Carbone, P. Baum, P. Rudolf, and A. H. Zewail, Phys. Rev. Lett. **100**, 035501, 2008.
6. S. Ghosh, S. M. Bachilo, R. A. Simonette, K. M. Beckingham, and R. B. Weisman, Science **330**, 1656, 2010.
7. G. Onida *et al.*, Rev. Mod. Phys. **74**, 601, 2002.
8. M. Rohlfing, Phys. Rev. Lett. **108**, 087402, 2012.

9. M. Rohlfing and S. G. Louie, Phys. Rev. B **62**, 4927, 2000.
10. C. D. Spataru *et al.*, Phys. Rev. Lett. **92**, 077402, 2004.
11. E. Chang *et al.*, Phys. Rev. Lett. **92**, 196401, 2004.
12. J. Maultzsch *et al.*, Phys. Rev. B **72**, 241402, 2005.
13. C. D. Spataru and F. Leonard, Phys. Rev. Lett. **104**, 177402, 2010.
14. M. Rohlfing, Phys. Rev. B **82**, 205127, 2010.
15. A. Greuling *et al.*, Phys. Rev. B **84**, 125413, 2011.
16. J. M. Garcia-Lastra and K. S. Thygesen, Phys. Rev. Lett. **106**, 187402, 2011.
17. A. Borghesi and G. Guizzetti, in *Handbook of optical constants of solids II*, edited by E.D. Palik, Academic Press, Boston, 1991.
18. V. N. Strocov, P. Blaha, H. I. Starnberg, M. Rohlfing, R. Claessen, J.-M. Debever, and J.-M. Themlin, Phys. Rev. B **61**, 4994, 2000.
19. V. N. Strocov, A. Charrier, J.-M. Themlin, M. Rohlfing, R. Claessen, N. Barrett, J. Avila, J. Sanchez, and M.-C. Asensio, Phys. Rev. B **64**, 075105, 2001.
20. A. Grüneis *et al.*, Phys. Rev. Lett. **100**, 037601, 2008.
21. A. Grüneis, C. Attaccalite, L. Wirtz, H. Shiozawa, R. Saito, T. Pichler, and A. Rubio, Phys. Rev. B **78**, 205425, 2008.
22. P. E. Trevisanutto, C. Giorgetti, L. Reining, M. Ladisa, and V. Olevano, Phys. Rev. Lett. **101**, 226405, 2008.
23. L. Yang, J. Deslippe, C.-H. Park, M. L. Cohen, and S. G. Louie, Phys. Rev. Lett. **103**, 186802, 2009.